Published in Surface Review and Letters (SRL) 9, issue 1, 235-240, 2002
which should be used for any reference to this work

ANGLE-SCANNED PHOTOEMISSION ON YbH_x: RELEVANCE FOR SWITCHABLE MIRRORS

J. HAYOZ, C. KOITZSCH, D. POPOVIĆ, M. BOVET, D. NAUMOVIĆ and P. AEBI*
Institut de Physique, Université de Fribourg, Pérolles, CH-1700 Fribourg, Switzerland

Yttrium, lantanum and rare earth elements can be loaded with hydrogen inducing a metal–insulator transition and giving rise to optical switching from reflecting to transparent. We present angle-scanned photoemission experiments characterizing thin YbH_x films grown on W(110) at room temperature. Hydrogen loading is performed in an ultrahigh-vacuum-compatible high pressure (1 bar) reaction cell. Via full-hemispherical X-ray photoelectron diffraction and low energy electron diffraction, it is demonstrated that these films grow well-ordered and single-crystalline. Ultraviolet photoemission reveals a gap for the dihydride phase confirming a transition from reflecting to transparent as seen by visual inspection. Ion implantation through additional H+ sputtering allows one to increase the hydrogen content to $x \approx 2.4$.

1. Introduction

The switchable optical properties of some metal hydrides[1] and also their hydrogen storage capabilities are of strong interest with respect to applications. Mostly trivalent elements such as Y and La have been used to induce optical switching at room temperature (RT) and with hydrogen pressures of the order of 1 bar. In Y, for instance, the metallic dihydride phase is loaded with hydrogen where, at $x \approx 2.85$ H atoms per formula unit, the material turns transparent. However, the physics behind putting hydrogen into a material is still not well understood. With hydrogen a proton and an electron are added to the metal host. This results in doping the host material and the understanding of doping is one of today's central problems in solid state physics. It has been realized that state-of-the-art *ab initio* local density approximation calculations do not reproduce the optical gap necessary to explain the transparent state in the tryhydride phase.[2] Other models, based on strong electron correlations, have been proposed to explain the metal–insulator transition.[3,4] There is an interesting and appealing connection between these models and the Zhang–Rice singlett[5] in high temperature superconductors (HT_c's). Hydrogen is suggested to be present in the form of H^-, one electron taken from the metal host. The two electrons on H^- are correlated but with drastically different radii around the proton. One electron is strongly bound to the proton whereas the other overlaps heavily with the metal d-states of the neighboring atoms. The two electrons form a singlett analogous to holes in the HT_c's. On the other hand, very recent GW calculations[6,7] demonstrate the formation of a sufficient gap to explain the metal–insulator transition without the need for strong electron correlations.

Indeed, detailed angle-resolved photoemission (ARPES) experiments are needed to favor one or the other model. However, practically all previous work on metal hydrides has been done on polycrystals and/or on samples that are capped with a protective Pd layer. In order to perform ARPES experiments, uncapped single crystalline material is needed. Furthermore, preparation has to take place *in situ* since Y, La and the rare earth used so far are extremely reactive. It is therefore important to explore how to prepare single crystalline hydrid films and to

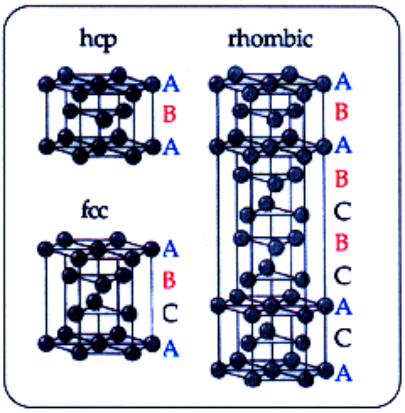

Fig. 1. Possibilities of close-packed layer stacking. Indicated are the sequences for hexagonal close-packed (hcp) face-centered cubic (fcc) and rhombic structures with characteristic layers A, B and C (from Ref. 10).

characterize them with respect to both the geometrical and the electronic structure. Recently, we were able to prepare thin, single crystalline Y films on W(110) and to load them with hydrogen.[8,9] The W(110) surface represents a quasihexagonal template inducing the growth of close-packed layers. Different sequences are possible (see Fig. 1) between the purely face-centered (fcc) and hexagonal close-packed (hcp) stacking with ABCABC... and ABAB... layers, respectively. The rhombic structure, for instance, can be viewed as a mixture of fcc and hcp stacking.

Since it is necessary to apply significant H partial pressures [compared to ultrahigh vacuum (UHV)] in order to reach the different hydride phases, we constructed a UHV-compatible high pressure (1 bar) cell.[9]

Here we present results on the preparation and characterization of thin single crystalline Yb films. Up to now switching to the transparent state has been induced in trivalent materials while increasing hydrogen pressure between the dihydride and the trihydide phase. Yb is divalent and the localized 4f electrons have a similar binding energy to the valence bandwidth, giving rise to an unstable 4f configuration.

The expectation is that it may be possible to have a reversed behavior for Yb thin films, i.e. the dihydride insulating and transparent and the transformation into the mirror (metallic) state induced by either reducing or increasing the hydrogen concentration.

We find that thin Yb films grown at RT on W(110) are single-crystalline and of hcp structure. Hydrogen loading is more difficult than for Y. Upon exposure to 1 bar of hydrogen the dihydride phase is formed exhibiting a characteristic gap in the valence band spectrum. Ion implantation via H^+ sputtering increases the near surface hydrogen concentration, x, to $x \approx 2.4$ and the spectra are indicative for a mixed valent phase which is reported to be metallic again.[11]

2. Experimental

The experiments were performed in a VG ESCALAB Mk II spectrometer with a base pressure $\leq 5 \cdot 10^{-11}$ mbar. The sample stage is modified for motorized sequential angle-scanned data acquisition over 2π solid angle.[12,13] MgK_a (1254.6 eV) and SiK_a (1740 eV) radiation is used for X-ray photoelectron spectroscopy (XPS) and X-ray photoelectron diffraction (XPD). The data acquisition mode to collect full-hemispherical XPD data is described in detail elsewhere.[14] Ultraviolet photoemission measurements were performed with monochromatized HeIα (21.2 eV) and He II (40.8 eV) radiation. The setup of the plasma discharge lamp with monochromator is presented in Ref. 15. The W(110) surface was prepared in UHV by flashing to 2500 K. After flashing, the W crystal was left in UHV for at least 5 h to reach room temperature. Yb was then evaporated by resistive heating of a Ta basket. Approximately 200-Å-thick films were grown within 30 min. The coverage was monitored with a quartz crystal oscillator. During deposition the pressure did not exceed 10^{-9} mbar. For all the films presented below the oxygen contamination as measured with XPS was below the detection limit and the W signal was not detectable anymore. In order to vary the H concentration, deposition was done under H_2 partial pressure and the films were exposed to 1 bar purified H_2. Details of the hydrogen pressure cell are presented elsewhere.[9] Briefly, highest purity H_2 for all hydrogen treatments of the films was produced via permeation through a Ag–Pd filter tube where the downstream side never comes in contact with non-UHV environment.

3. Results and Discussion

Figure 2 displays XPD patterns for differently prepared films. The XPD patterns allow a very

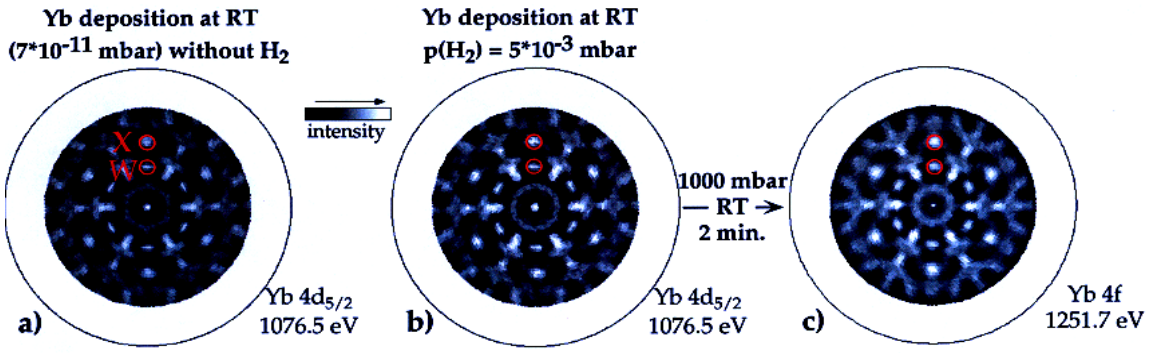

Fig. 2. Photoelectron diffraction patterns (sixfold-symmetry-averaged) for (a) a 200-Å-thick Yb film deposited on W(110) at room temperature (RT); (b) same as (a) but deposition under 5×10^{-3} mbar H_2 partial pressure; (c) same as (a) but deposited under 10^{-6} mbar H_2 partial pressure and subsequently exposed to 1000 mbar H_2. Photoelectron kinetic energies and deposition conditions are labeled. Points X and W mark specific forward focusing maxima.

simple interpretation in the case, such as here, of photoelectron kinetic energies above approximately 500 eV.[16] Photoelectrons leaving the emitter atom are strongly focused in the forward direction by the neighboring atoms. The measured intensities are therefore strongly enhanced along densely packed atomic rows and crystallographic planes. In this energy regime, the so-called forward focusing is only weakly dependent on the atomic number Z of scatterer atoms. Furthermore, it was shown in Ref. 13 based on a large data set that the final-state scattering produces patterns that are virtually independent of the initial state angular momentum.

Due to the limited mean free path of photoelectrons, the angular intensity distribution measured in the forward focusing regime is characteristic of the near surface crystallography. Via comparison with angular distributions taken from known structures, the identification of unknown systems is possible.[17]

The intensity of the Yb $4d_{5/2}$ and 4f photoemission lines have been measured as a function of emission angle and mapped stereographically in a linear gray scale representation (Fig. 2). High and low intensities are drawn in white and black, respectively. Normal emission corresponds to the center of the plot whereas emission parallel to the surface, i.e. 90° polar emission angle, is indicated by the outer circle.

For the measurement shown in Fig. 2(a), Yb was deposited in UHV at RT, whereas for Fig. 2(b) the film was deposited at RT but under a H_2 partial pressure of 5×10^{-3} mbar. The patterns of the two films look very similar and can be identified as Yb layers with hcp stacking. The XPD pattern of close-packed layers with fcc stacking, as found in the case of YH_2 (not shown), is distinctly different.[8] The finding of hcp stacking for Yb deposition on W(110) at RT is in contradiction to the fcc stacking reported by Weschke *et al.*[18] The reason might be that Yb exhibits a transition from hcp to fcc below RT,[19,20] and therefore is intrinsically unstable with respect to different stackings. Note also that single crystalline Yb films deposited at RT on saphire (11–20) exhibit fcc stacking (not shown).

An additional exposure to 1 bar of H_2 applied to a film grown under 10^{-6} mbar H_2 partial pressure results in a pattern such as shown in Fig. 2(c). The contrast is slightly degraded but the intensity distribution is still very similar. Differences are due to a roughening of the film (see below) and also to an admixture of non-hcp stacking, i.e. a rhombic structure. From bulk polycrystals it is known that Yb forms a nonmetallic, rhombic dihydride phase.[11] Since photoelectrons have a finite escape depth, several layers are sampled and the exact stacking sequence, i.e. the amount of ABC stacking admixture, cannot be identified with precision. In addition the situation is complicated by the presence of differently oriented domains. However, the measurement clearly indicates strong hcp stacking character.

The distinct high intensity features in Fig. 2, labeled W and X, originate from close-lying emitter–scatterer directions characteristic of the stacking. The corresponding emission angles are determined by the c/a ratio, where a and c are the in- and out-of-

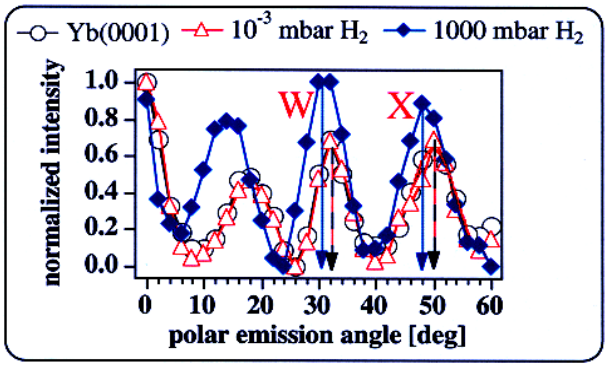

Fig. 3. Polar scans across characteristic forward forcusing maxima indicated in Fig. 2. The maxima shift for the different films, indicating a change in interlayer spacing.

plane lattice constants, respectively. A closer analysis, shown in Fig. 3, manifests a decreased emission angle and therefore an increased c/a ratio for the 1 bar H_2 exposed film [Fig. 2(c)]. The increase of c/a amounts to roughly 8%.

In order to get information on the in-plane lattice constant, a, and consequently on the interlayer expansion, and also on the long range order quality of the films, we performed LEED experiments. Figure 4(a) shows the diffraction spots of the Yb film deposited at RT in UHV, recorded for a primary electron energy of 80 eV. The spots are sharp and well defined, indicative of a well-ordered film. In Fig. 4(b) we display the pattern for a Yb film deposited under a H_2 partial pressure of 5×10^{-3} mbar. The film remains equally well ordered. For an exposure to 1 bar H_2, however, a certain loss of long range order is observed in Fig. 4(c). The distance between the diffraction spots (marked by a white arrow in Fig. 4) gives a measure for the in-plane distance. Going from Fig. 4(a) to 4(b), no change is observed. In Fig. 4(c), however, the distance between the diffraction spots slightly increases, indicating a decrease of the in-plane lattice constant by approximately 2%.

Together with the result for the c/a ratio from XPD (8% increase) we find an interlayer expansion of approximately 6excellent agreement with the expansion of 6%, reported for YbH_2.[10] Therefore, XPD and LEED together give evidence for the formation of the dihydride. The films stay single-crystalline (XPD) but there is a certain loss of long range order (LEED). Note that a similar treatment applied to Y films already induces the trihydride phase.[9]

The next step is to consider the photoemission spectra of the Yb 3d emission line which is susceptible to the valence of Yb. The removal of a 3d electron in the divalent case results in a single line, which is only broadened by lifetime and instrumentals effects. For trivalent Yb the hole in the 4f shell (induced through the promotion of a 4f electron into the valence band) together with the 3d hole created by the photoemission process results in a rather broad multiplet structure. Figure 5 displays the spectra of the different films. Labeled with (a) and (b) are films deposited in UHV and under a H_2 partial pressure of 5×10^{-3} mbar, respectively. No significant differences are noticed. The two ticks mark a bulk and surface plasmon/band transition[11,21] and are not

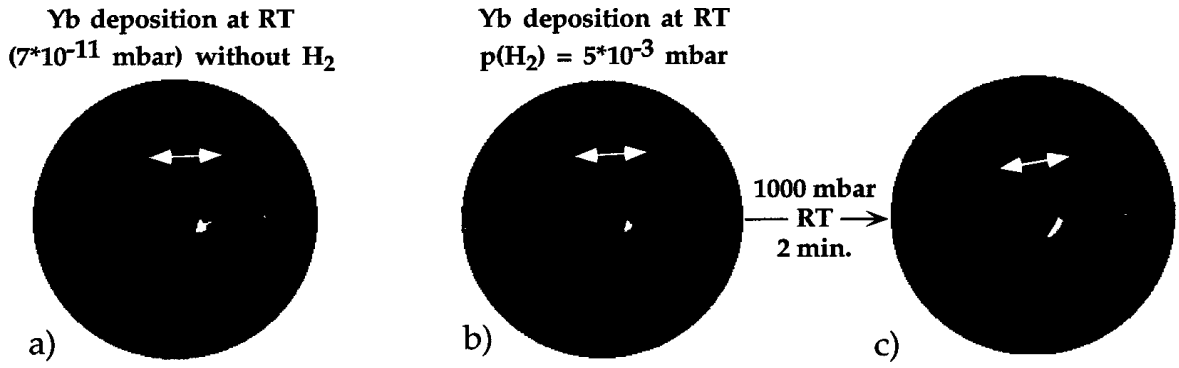

Fig. 4. Low energy electron diffraction pattern ($E_0 = 80$ eV) for (a) a 200-Å-thick Yb film deposited on W(110) at room temperature (RT); (b) same as (a) but deposition under 5×10^{-3} mbar H_2 partial pressure; (c) same as (a) but deposited under 10^{-6} mbar H_2 partial pressure and subsequently exposed to 1000 mbar H_2. White arrows indicate the distance between two diffraction spots indicative of in-plane lattice constant changes.

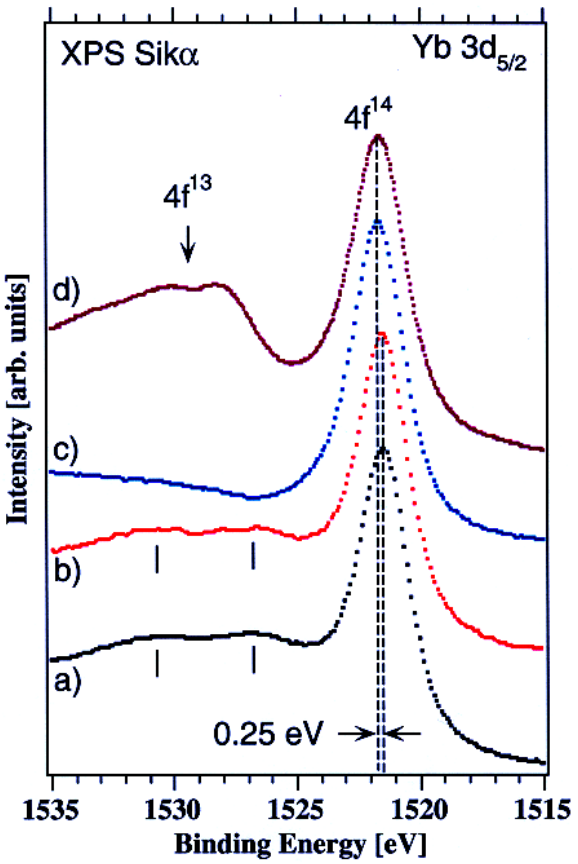

Fig. 5. SiKα excited Yb3d$_{5/2}$ photoemission line for (a) a 200-Å-thick Yb film deposited on W(110) at room temperature (RT); (b) same as (a) but deposition under 5×10^{-3} mbar H_2 partial pressure; (c) same as (a) but deposited under 10^{-6} mbar H_2 partial pressure and subsequently exposed to 1000 mbar H_2; (d) a 200-Å-thick Yb film deposited on sapphire (11–20) at RT and subsequently H^+-sputtered.

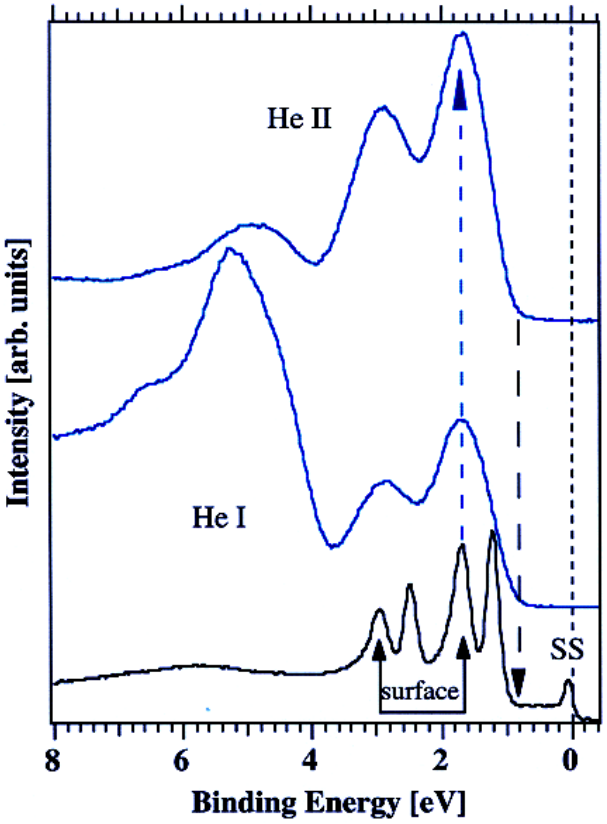

Fig. 6. Normal emission photoemission spectra of 200-Å-thick Yb films grown on W(110) at room temperature. (*Bottom*) Pure Yb measured with HeI radiation, (*middle*) Yb film deposited under 10^{-6} mbar H_2 and subsequently exposed to 1000 mbar H_2, measured with HeI, (*top*) same as (*middle*) but measured with HeII radiation.

present anymore in the dihydride [spectrum (c)] which is insulating (see below). For spectrum (c) the film has been exposed, in addition to deposition under 10^{-6} mbar H_2, to 1 bar H_2 for 2 min. The spectrum is very similar to spectra of polycrystalline samples with a concentration of $x = 2.0$.[11,21,22] These polycrystalline samples have been calibrated very carefully with volumetric methods by dissolving them in dilute HCl.[11] Therefore, the films corresponding to spectrum (c) are close to YbH_2 confirming our findings with XPD and LEED. Spectrum (d) represents a film deposited on sapphire (11–20) and, in addition, has been sputtered with H^+ (4.5 keV, 60 μA) for 5 min. The split shoulder at higher binding energy is characteristic of f^{13} final state multiplets and therefore of a mixed valent phase. A comparison with data taken on polycrystalline samples[11,21,22] indicates that we reached approximately $YbH_{2.4}$, a composition reported to be metallic.[11] The film of spectrum (d), however, becomes completely disordered, as seen from XPD and LEED (not shown).

In order to access the electronic structure directly, valence band spectra have been recorded. Figure 6 shows normal emission data taken with HeI ($h\nu = 21.2$ eV) (two bottommost spectra) and HeII ($h\nu = 40.8$ eV) (topmost spectrum) radiation. For Yb metal (bottommost spectrum) with a $4f^{14}$ ground state configuration, $4f^{13}$ photoemission final state doublets are observed, split into $4f_{7/2}$ and $4f_{5/2}$ lines. Each line consists of two components due to contributions from bulk and surface atoms separated

by the so-called surface core level shift.[23] The sharp peak close to zero binding energy (Fermi level) is the well-known surface state present on many close-packed rare earth surfaces.[24] For the film which is evaporated under a H_2 partial pressure of 10^{-6} mbar and subsequently exposed to 1 bar of H_2 (center and top spectrum) the electronic states near the Fermi level completely disappeared, indicating the opening of the gap and the metal–insulator transition. A visual inspection of a film prepared under the same conditions on (transparent) sapphire indicates that it becomes transparent. Thus, the YbH2 films are insulating and transparent.

In addition, the surface-induced splitting of the 4f states has disappeared but the binding energy positions of the maxima are centered at the surface-shifted core levels. This behavior can be attributed to a roughening of the surface induced by the loading of the film under 1 bar of H_2. A variety of different Yb surface atom environments are created with different core level shifts, leading to the broadening. This broadening is consistent with the loss of long range order as observed by LEED in Fig. 4(c).

Furthermore a broad feature has appeared at about 5.5 eV binding energy. This feature can be attributed to hydrogen-induced states since the HeII spectrum taken on the same films (topmost spectrum) shows a strong relative weight increase of the f-states with respect to the 5.5 eV maximum. Therefore it is not of 4f character, for example induced through a valence change. It is also not a fingerprint of oxygen contamination since it would also have appeared in the O 1s XPS and O-contaminated films exhibit a valence band feature centered at 6 eV.

4. Conclusions

In summary, we have demonstrated that Yb, at RT, grows with hcp stacking on W(110). Loading with 1 bar of H_2 results in the dihydride as indicated by the increased interlayer spacing, the comparison with published XPS data of polycrystalline samples and the opening of the gap in the normal emission valence band spectra. Deposition under a H_2 partial pressure of 5×10^{-3} mbar almost does not induce changes, clearly indicating that hydrogenation of Yb is more difficult than for example for Y. Ion implantation via H^+ sputtering results in a mixed valent YbH_x phase with $x \approx 2.4$, which is metallic again. Therefore Yb definitely offers the possiblity of inducing a metal–insulator transition via both H content increase and decrease.

The formation of the dihydride phase results in a considerable roughening of the surface manifested in broadened LEED spots and an increased intensity and broadening of the surface component of the 4f lines.

Acknowledgments

Skillful technical assistance was provided by E. Mooser, O. Raetzo, Ch. Neururer and F. Bourqui. This project has been supported by the Fonds National Suisse de la Recherche Scientifique.

References

1. J. N. Huiberts, R. Griessen, J. H. Rector, R. J. Wijngaarden, J. P. Dekker, D. G. de Groot and N. J. Koemann, *Nature* **380**, 231 (1996).
2. P. J. Kelly, J. P. Dekker and R. Stumpf, *Phys. Rev. Lett.* **78**, 1315 (1997).
3. R. Eder, H. F. Pen and G. A. Sawatzky, *Phys. Rev.* **B56**, 10115 (1997).
4. K. K. Ng *et al.*, *Phys. Rev. Lett.* **78**, 1311 (1997).
5. F. C. Zhang and T. M. Rice, *Phys. Rev. Lett.* **37**, 3759 (1988).
6. T. Miyake, F. Aryasetiawan, H. Kino and K. Terakura, *Phys. Rev.* **B61**, 16491 (2000).
7. P. van Gelderen, P. A. Bobbert, P. J. Kelly and G. Brocks, *Phys. Rev. Lett.* **85**, 2989 (2000).
8. J. Hayoz, S. Sarbach, Th. Pillo, E. Boschung, D. Naumovic, P. Aebi and L. Schlapbach, *Phys. Rev.* **B58**, R4270 (1998).
9. J. Hayoz, Th. Pillo, M. Bovet, A. Züttel, St. Guthrie, G. Pastore, L. Schlapbach and P. Aebi, *J. Vac. Sci. Tech.* **A18**(5), 2417 (2000).
10. P. Vajda, in *Handbook on the Physics and Chemistry of Rare Earths*, eds. K. A. Gschneider and L. Eyring, Vol. 20 (Elsevier, Amsterdam, 1995).
11. S. Büchler, PhD thesis, Swiss Federal Institute of Technology, Switzerland (1989).
12. J. Osterwalder, T. Greber, A. Stuck and L. Schlapbach, *Phys. Rev.* **B47**, 13764 (1991).
13. D. Naumović, A. Stuck, T. Greber, J. Osterwalder and L. Schlapbach, *Phys. Rev.* **B47**, 7462 (1993).
14. R. Fasel, P. Aebi, J. Osterwalder, L. Schlapbach, R. G. Agostino and G. Chiarello, *Phys. Rev.* **B50**, 14516 (1994).
15. Th. Pillo, L. Patthey, E. Boschung, J. Hayoz, P. Aebi and L. Schlapbach, *J. Electr. Spectrosc. Relat. Phenom.* **97**, 243 (1998).
16. C. S. Fadley, in: R. T. Bachrach, ed., *Synchrotron Radiation Research: Advances in Surface Science*, Vol. 1 (Plenum, New York, 1990).

17. Th. Pillo, J. Hayoz, P. Schwaller, H. Berger, P. Aebi and L. Schlapbach, *Appl. Phys. Lett.* **75**, 1550 (1999).
18. E. Weschke, A. Yu. Grigoriev, C. Schüssler-Langeheine, C. Mazumdar, R. Meier, S. Vandré, S. Ram, L. Kilian, G. Kaindl and C. Sutter, *Phys. Rev. Lett.* **83**, 584 (1999).
19. E. Bucher, P. H. Schmidt, A. Jayaraman, K. Andres, J. P. Maita, K. Nassau and P. D. Dernier, *Phys. Rev.* **B2**, 3911 (1970).
20. F. X. Kayser, *Phys. Rev. Lett.* **25**, 662 (1970).
21. S. Büchler, R. Monnier and L. Degiorgi, L. Schlapbach, *Zeitschrift für Physikalische Chemie Neue Folge* **163**, 579 (1989).
22. S. Büchler, L. Schlapbach, R. Monnier and L. Degiorgi, *Journal de Physique, Suppl. 12* **48**, C9–947 (1987).
23. G. Kaindl, A. Höhr, E. Weschke, S. Vandré, C. Schüssler-Langeheine and C. Laubschat, *Phys. Rev.* **B51**, 7920 (1995).
24. M. Bodenbach, A. Höhr, C. Laubschat, G. Kaindl and M. Methfessel, *Phys. Rev.* **B50**, 14446 (1994).